Differential Regulation of Six Heavy Metal Efflux Systems in the Response of *Myxococcus xanthus* to Copper[▽][†]

Aurelio Moraleda-Muñoz, Juana Pérez, Antonio Luis Extremera, and José Muñoz-Dorado*

Departamento de Microbiología, Facultad de Ciencias, Universidad de Granada, Avda. Fuentenueva s/n, E-18071 Granada, Spain

Myxococcus xanthus has to cope with changes in its environment during growth and development. Among these factors, the concentration of copper is crucial due to the essential toxic effect of this metal, which forces the cells to maintain a tight homeostasis. The *M. xanthus* copper response is more complex than that in other bacteria, which is reflected by the different copper sensitivities of growing and developing cells. In the present study, the participation in copper homeostasis of six heavy metal efflux systems encoded in the *M. xanthus* genome has been examined. Three of these pumps exhibit the signature sequences in transmembrane domain 4 of the Cus systems (Cus1, Cus2, and Cus3), while the other three exhibit the motifs of the Czc systems (Czc1, Czc2, and Czc3). The Cus2 and Cus3 systems are inducible by copper and monovalent metals, functioning as the main copper efflux pumps, while the Cus1 system is implicated in Zn^{2+} homeostasis. The Czc systems are also differentially regulated either by divalent metals but not by copper (Czc1), by copper and divalent metals (Czc2), or by starvation (Czc3). The differential regulation of these six efflux systems ensures the proper completion of the *M. xanthus* life cycle in an environment with fluctuating concentrations of copper and other metals.

Myxococcus xanthus is a rod-shaped deltaproteobacterium considered a model to study social behavior in prokaryotes. *M. xanthus* cells are found in the topsoil, where they cooperatively feed on decaying organic matter and prey on other microorganisms. However, upon starvation, a developmental process initiates, consisting of the formation of multicellular mound-shaped structures called fruiting bodies, inside which cells differentiate into dormant spherical myxospores. The spores in a fruiting body can germinate and resume growth when nutrients become available (35).

In their habitats, cells have to deal with fluctuations in levels of several metal ions (19). Copper is a crucial trace transition metal required for a number of enzymes involved in energy metabolism and cell detoxification (24) but can cause serious damage through the formation of reactive oxygen species at high concentrations (4, 34). Thus, copper homeostasis has to be tightly regulated to prevent toxic effects. One of the mechanisms that bacteria use to protect themselves from the toxic effect of copper is the active efflux of metals. Two main detoxification mechanisms are known to function in Gram-negative bacteria: (i) P_{1B}-type ATPases, which use ATP energy to pump Cu^+ out of the cytoplasm to the periplasm (1), where multicopper oxidases (MCOs) will oxidize this Cu^+ to the less toxic form Cu^{2+} (30), and (ii) CBA transporters (consisting of subunits C, B, and A), which extrude metals from the cytoplasm or the periplasm to outside the outer membrane (5, 9, 22).

The central pump protein of the CBA transporters belongs to the resistance-nodulation-cell division (RND) family, which functions as a transporter energized by proton-substrate antiport (6, 20, 27, 32). The other two components are an outer membrane factor (OMF), which enters into the periplasm and produces an exit duct, and a membrane fusion protein (MFP), which acts as an adaptor to stabilize the contact between the RND and the OMF components. Bacterial CBA efflux systems span the complete cell wall of a Gram-negative bacterium from the cytoplasm to the exterior. Accordingly, they must be able to catalyze transenvelope efflux (from the cytoplasm directly to the exterior), outer membrane efflux (from the periplasm to the outside), or both processes. CBA systems are involved in the export of metal ions, xenobiotics, and drugs, depending on the characteristics of the individual RND protein. The members of this superfamily involved in the transport of hydrophobic and amphiphilic compounds are designated HAE-RND, and those that efflux heavy metals are designated HME-RND (32). The latter family includes pumps that export monovalent metals, known as Cus systems (for Cu sensing), and those that export divalent metals, named Czc systems (for cobalt, zinc, and cadmium). Transmembrane segment 4 (TM4) of monovalent metal RND transporters distinctively differs in sequence from those transporting divalent metal cations or organic compounds (26).

The *M. xanthus* copper response seems to differ from those described for other bacteria on the basis of several observations. First, developmental cells are more sensitive to copper than are growing cells, since concentrations higher than 900 μM and 60 μM are lethal for growing and developing cells, respectively (30). However, copper-preadapted cells are as resistant to this metal during development as they are during growth, suggesting the induction of several mechanisms that confer metal resistance. Second, copper induces the production of carotenoids in cultures grown in the dark (16). Finally, *in silico* studies of the complete genome of *M. xanthus* have

* Corresponding author. Mailing address: Departamento de Microbiología, Facultad de Ciencias, Universidad de Granada, Avda. Fuentenueva s/n, E-18071 Granada, Spain. Phone: (34) 958243183. Fax: (34) 958249486. E-mail: jdorado@ugr.es.

revealed the presence of a large number of gene products with sequence similarities to proteins previously reported for other bacteria to be involved in copper detoxification, all of which are redundant. We have identified three MCOs (30), three P_{1B}-type ATPases (15), and six CBA transporters of the HME-RND group. The great abundance of paralogous genes involved in copper resistance would seem to be contradictory with the copper sensitivity of *M. xanthus*; that is, several bacteria (such as *Escherichia coli*) that encode only one of each of these elements are more resistant to copper than *M. xanthus* (26, 30). This observation raises the question of why *M. xanthus* holds so many paralogous genes to confer copper resistance.

We started the analysis of the *M. xanthus* global copper response by exploring the family of paralogs of the MCOs, which includes CuoA, CuoB, and CuoC (30). We continue the study by investigating the six HME-RND pumps, three of which exhibit the consensus sequence in TM4 of the Cus systems (designated Cus1, Cus2, and Cus3) and the other three of which exhibit the signature of the Czc systems (named Czc1, Czc2, and Czc3). We have found that these six systems are differentially regulated by copper, other metals, and/or starvation. Some of them are essential for cell viability in the presence of high copper concentrations, and others are essential for the completion of development, even in the absence of external copper.

MATERIALS AND METHODS

Identification of CBA systems in the *M. xanthus* genome. Genes encoding CBA transporters in the *M. xanthus* genome were identified by BLASTP analysis using the sequences of the *E. coli* proteins CusA (GenBank accession number NP_415107) (RND), CusB (accession number NP_415106.1) (MFP), and CusC (accession number NP_415104.1) (OMF). All sequences obtained with an E value of <3 were back-searched against the NCBI database (http://blast.ncbi.nlm .nih.gov/) to confirm similarities to the corresponding subunits of the CBA systems and against the Pfam database (3) to verify that they matched Pfam accession numbers PF00873 (AcrB/AcrD/AcrF family), in the case of the RND proteins, and PF02321 (outer membrane efflux protein), in the case of the OMF proteins. In addition, genes located adjacent to all the genes identified as belonging to CBA systems were also analyzed. Prediction of transmembrane domains and subcellular localization of the proteins were carried out with the TMHMM (http://www.cbs.dtu.dk/services/TMHMM-2.0/) and SOSUI (http://bp .nuap.nagoya-u.ac.jp/sosui/) servers. The consensus sequences in TM4 of the RND proteins were manually analyzed.

Bacterial strains, plasmids, and culture conditions. Bacterial strains and plasmids used in this study are listed in Table S1 in the supplemental material. All *M. xanthus* strains were grown at 30°C with vigorous shaking (300 rpm) in CTT broth (10). CTT agar plates contained 1.5% Bacto agar (Difco). When necessary, kanamycin (80 μg ml^{-1}), X-Gal (5-bromo-4-chloro-3-indolyl-β-D-galactopyranoside) (100 μg ml^{-1}), or galactose (10 mg ml^{-1}) was added. When required, CTT medium was supplemented with metals at the concentrations indicated in the figure legends and tables. Luria-Bertani broth (28), supplemented with kanamycin (25 μg ml^{-1}) or X-Gal (25 μg ml^{-1}) when needed, was used to grow *E. coli* strains at 37°C. Standard protocols were followed for nucleic acid manipulations (28).

Construction of in-frame deletion mutants. The in-frame deletion strains were generated by allelic exchange using the GalK selection method (33). Briefly, sequences upstream and downstream of the genes constituting HME-RND systems were amplified by PCR with PrimeSTARHS high-fidelity polymerase (Takara), using wild-type (WT) chromosomal DNA as a template and the primers listed in Table S2 in the supplemental material. The amplified products were then cloned into KpnI- and HindIII-digested pBJ113 (11) to obtain plasmids harboring deletions of the corresponding CBA transporter (Table S1). The resulting nonreplicating plasmids carrying the deletions were introduced into *M. xanthus* cells by electroporation (12). Chromosomal integration was selected by plating cells onto CTT plates containing 80 μg ml^{-1} kanamycin (positive selection). Several randomly chosen kanamycin-resistant (Km^r) merodiploids were

analyzed by Southern blot hybridization for the proper recombination event. One positive strain was then grown in the absence of kanamycin and plated onto CTT plates containing 1% galactose for negative selection. Southern blot analysis was used to screen kanamycin-sensitive (Km^s) and galactose-resistant (Gal^r) colonies, searching for the loss of the WT allele.

Development. The starvation medium CF (8) was used to induce development, which was supplemented with metals at the concentrations indicated in the figure legends and tables when needed. Cells were grown in CTT broth to approximately 3.0×10^8 cells ml^{-1} (optical density at 600 nm [OD$_{600}$] of 1) and resuspended to 4.5×10^9 cells ml^{-1} (OD$_{600}$ of 15) in TM buffer (10 mM Tris-HCl [pH 7.6], 1 mM MgSO$_4$). Ten microliters of each suspension was spotted onto CF agar plates and incubated at 30°C, with observation on a Wild Heerbrugg dissecting microscope.

Construction and assay of strains harboring *lacZ* fusions. The *lacZ* fusion plasmids were constructed by using vector pKY481 (2). By use of PrimeSTARHS polymerase (Takara), fragments encompassing the upstream CBA transporter regions were amplified from WT chromosomal DNA by the use of the oligonucleotide pairs indicated in Table S2 in the supplemental material. The BamHI site in the primers was introduced at the start codon of the first *cus/czc* system gene and in frame with the BamHI site existing in the *lacZ* gene of plasmid pKY481. PCR products were digested with KpnI and BamHI and ligated into vector pKY481 digested with the same enzymes. The resulting plasmids were introduced into *M. xanthus* cells by electroporation, and the Km^r colonies were analyzed by Southern blotting.

Strains containing *lacZ* fusions were incubated at 30°C on CTT and CF agar plates containing different metal concentrations. For qualitative analyses of β-galactosidase activity, plates containing 100 μg ml^{-1} of X-Gal were used. For quantitative analyses, cell extracts were obtained at different times by sonication and assayed for activity as previously reported (16). The amount of protein in the supernatants was determined by using the Bio-Rad protein assay (Bio-Rad, Inc.) with bovine serum albumin as a standard. β-Galactosidase activity was determined as described previously by Kroos et al. (13). Specific activity is expressed as nmol of *o*-nitrophenol produced per min and mg of protein. The results are the averages of data from three different experiments.

RESULTS

CBA systems in the *M. xanthus* genome. A search for CBA transporters in the *M. xanthus* genome has revealed the presence of 14 genes that encode proteins with similarities to the RND component, 17 with similarities to MFP, and 14 with similarities to OMF (see Fig. S1 in the supplemental material). By analyzing the sequence motifs in TM4 of all of the RND-like proteins, it was possible to classify six systems into the HME-RND family. Three of these RND proteins have the conserved motif AX_5DX_6E, which is present in the monovalent metal cation transporters (26). These systems have been designated Cus1, Cus2, and Cus3. The three subunits of each system (RND, MFP, and OMF) are encoded by adjacent genes (Fig. 1B and E). The other three RND proteins contain the consensus motif DX_5DX_6E, typical of those systems involved in the trafficking of divalent metal cations (26). For that reason, these three systems have been named Czc1, Czc2, and Czc3 (Fig. 1C, D, and F). Two of them, Czc1 and Czc3, are composed of the three above-mentioned subunits encoded by contiguous genes (Fig. 1C and F). In contrast, only the subunits RND and MFP of the Czc2 system are encoded together in the chromosome (Fig. 1D). Nevertheless, as several OMF-like proteins are found as orphans in the genome (Fig. S1), it is plausible to speculate that they might function with the subunits CzcA2 and CzcB2 to extrude metals to the exterior. The rest of the RND proteins contain the sequence signature defined for those CBA systems involved in organic compound detoxification, or they could not be classified into any group because they do not contain any conserved motif (26). These systems have been excluded from this study.
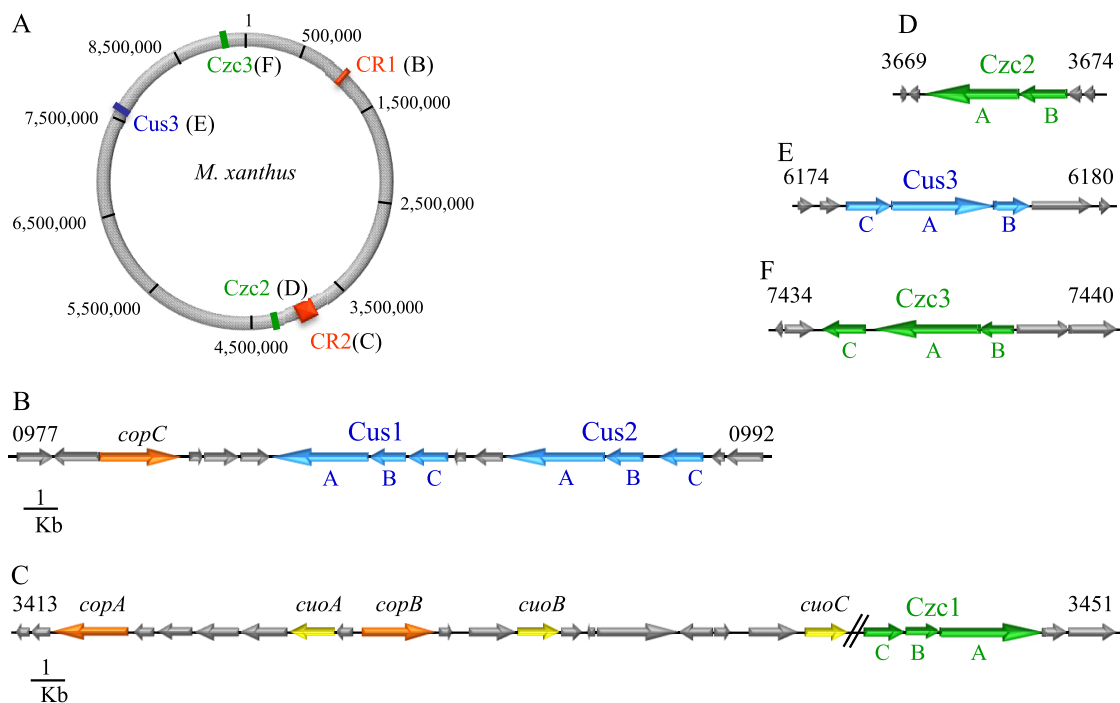
FIG. 1. Schematic depiction of the location of the six CBA efflux heavy metal systems in the *M. xanthus* genome. (A) *M. xanthus* genome map with the positions of copper region 1 (CR1), copper region 2 (CR2), and the dispersed *czc2*, *cus3*, and *czc3* systems. (B) Genes located in copper region 1. (C) Genes located in copper region 2. (D) Genetic environment of the *czc2* system. (E) Genetic environment of the *cus3* system. (F) Genetic environment of the *czc3* system. The numbers indicated at the top of the first and last genes in each panel correspond to their identifiers in the *M. xanthus* genome. Paralogous genes are represented with the same color. Blue, *cus* systems; green, *czc* systems; orange, P_{1B}-ATPases; yellow, MCOs. The rest of the genes are depicted as gray arrows.

The Cus1 and Cus2 systems are encoded very close in the chromosome, in a region that has been designated copper region 1, where the copper-dependent P_{1B}-ATPase CopC (15) is also found (Fig. 1A and B). Conversely, Czc1 is located in copper region 2 (Fig. 1C), along with the genes for the three MCOs (30) and the P_{1B}-type ATPases CopA and CopB (15). The Cus3, Czc2, and Czc3 systems are dispersed throughout the genome (Fig. 1D to F).

Expression of the HME-RND systems. The expression profiles of the *cus* and *czc* systems were examined during growth and development in *M. xanthus* strains harboring in-frame fusions between the first gene of each cluster and the *lacZ* gene from *E. coli*. These analyses revealed that the three *cus* systems exhibited undetectable or very low levels of β-galactosidase activity during growth in the absence of metals (Fig. 2). How-

ever, their expression levels increased in a time-dependent manner by the addition of external copper, although the levels reached by *cus2* and *cus3* were much higher than those reached by *cus1*. The three Cus systems responded more efficiently to low copper concentrations than to high copper concentrations (Fig. 2).

During development, the copper responses of the *cus* systems were analyzed by using a 10-fold-lower concentration of the metal to prevent cells from dying (30). During this stage, the expression of *cus1* was almost undetectable in the absence and in the presence of copper (Fig. 3A). In contrast, *cus2* and *cus3* responded to the copper supplementation in a manner different from that observed during growth (compare Fig. 2B and C with 3B and C, respectively). *cus2* increased its expression level in a time-dependent manner, reaching a plateau at
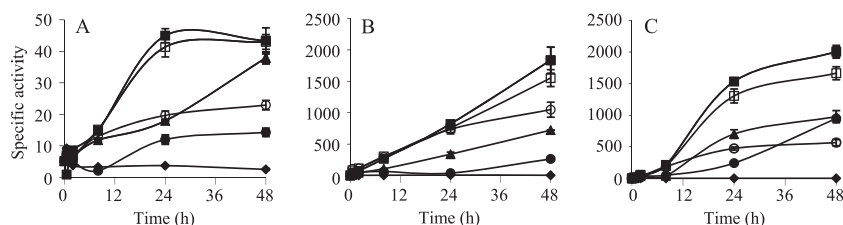

FIG. 2. Copper upregulation of *cus1* (A), *cus2* (B), and *cus3* (C) during growth. Strains were incubated on CTT agar plates containing 0 μM (◆), 50 μM (○), 150 μM (□), 300 μM (■), 600 μM (▲), or 800 μM (●) copper. The specific β-galactosidase activity in cell extracts was determined as described in Materials and Methods. The results are the averages of data from three different experiments. The error bars indicate standard deviations. Note the differences in the scales.
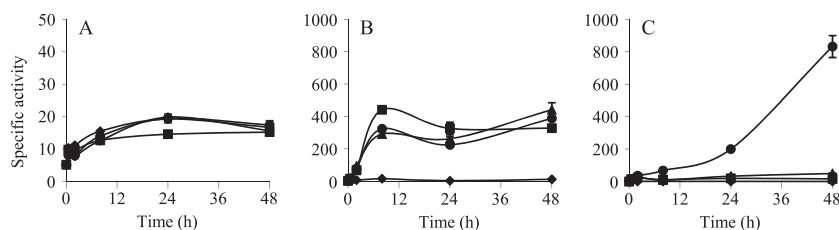
FIG. 3. Copper upregulation of *cus1* (A), *cus2* (B), and *cus3* (C) during development. Strains were incubated on CF agar plates containing 0 μM (◆), 20 μM (■), 40 μM (▲), or 60 μM (●) copper. The specific β-galactosidase activity in the cell extracts was determined as described in Materials and Methods. The results are the averages of data from three different experiments. The error bars indicate standard deviations. Note the differences in the scales.

8 h of starvation (Fig. 3B). In addition, the expression profiles did not exhibit a marked metal concentration dependency. The expression of *cus3* increased considerably only in response to copper concentrations of 60 μM and after a 24-h incubation (Fig. 3C).

Of the two redox states of copper, Cu^+ is the form that dominates in the reducing cell environment, while Cu^{2+} predominates outside the cytoplasm (4, 34). As these two redox states can be mimicked by monovalent and divalent metals, respectively, the expression of the *cus* systems in the presence of Au^+, Ag^+, Fe^{2+}, Mn^{2+}, Ni^{2+}, Zn^{2+}, Co^{2+}, and Cd^{2+} was

also analyzed. The strains harboring fusions were first tested on agar plates containing X-Gal and several concentrations of each metal, and those concentrations that gave the most intense blue color were chosen to quantify β-galactosidase activity. The results obtained showed that *cus1* expression levels were higher with Zn^{2+} than with copper (Table 1), indicating that this system could be involved in Zn^{2+} homeostasis. The *cus2* promoter responded mainly to copper and gold, suggesting that Cu^+ might be the inducer. Conversely, *cus3* was strongly induced by copper and Cd^{2+} (Table 1), pointing to an induction by Cu^{2+}. The other metals tested exerted scant or no

TABLE 1. Responses of *cus* promoters to heavy metals

CBA system	Inducer	Growth			Development		
		Metal concn (mM)	Avg β-galactosidase activity ± SD[b]	Fold induction[a]	Metal concn (mM)	Avg β-galactosidase activity ± SD[b]	Fold induction[a]
cus1	None		4 ± 0.1			19 ± 0.1	
	CuSO$_4$	0.3	45 ± 2	11	0.060	20 ± 0.2	1
	Ni(NO$_3$)$_2$	1.0	12 ± 0.5	3	2.0	46 ± 1	2
	Zn(NO$_3$)$_2$	0.25	207 ± 7	52	0.1	203 ± 8	11
	Co(NO$_3$)$_2$	0.5	7 ± 0.1	2	1.0	66 ± 2	4
	Cd(NO$_3$)$_2$	0.1	4 ± 0.3	1	0.025	9 ± 0.3	0.5
	FeSO$_4$	6.0	7 ± 1	2	6.0	118 ± 6	6.2
	MnSO$_4$	0.6	ND		0.8	ND	
	AgNO$_3$	0.1	3 ± 1	1	0.01	12 ± 1	0.6
	AuCl$_3$	1.0	7 ± 0.5	2	0.25	26 ± 1	1
cus2	None		7 ± 1			2 ± 0.1	
	CuSO$_4$	0.3	641 ± 5	92	0.020	326 ± 33	163
	Ni(NO$_3$)$_2$	1.0	ND		2.0	21 ± 2	11
	Zn(NO$_3$)$_2$	0.25	ND		0.1	6 ± 0.1	3
	Co(NO$_3$)$_2$	0.5	ND		1.0	20 ± 1	10
	Cd(NO$_3$)$_2$	0.1	37 ± 0.5	5	0.025	125 ± 2	63
	FeSO$_4$	6.0	4 ± 0.1	1	6.0	ND	
	MnSO$_4$	0.6	ND		0.8	ND	
	AgNO$_3$	0.1	20 ± 1	3	0.01	49 ± 1	25
	AuCl$_3$	1.0	637 ± 9	91	0.25	1,250 ± 59	625
cus3	None		1 ± 0.3			0.4 ± 0.2	
	CuSO$_4$	0.3	1,533 ± 12	1,533	0.060	200 ± 3	500
	Ni(NO$_3$)$_2$	1.0	ND		2.0	ND	
	Zn(NO$_3$)$_2$	0.25	ND		0.1	ND	
	Co(NO$_3$)$_2$	0.5	ND		1.0	ND	
	Cd(NO$_3$)$_2$	0.1	1,142 ± 8	1,142	0.025	878 ± 56	2,195
	FeSO$_4$	6.0	ND		6.0	ND	
	MnSO$_4$	0.6	ND		0.8	ND	
	AgNO$_3$	0.1	1 ± 0.3	1	0.01	76 ± 2	190
	AuCl$_3$	1.0	105 ± 3	105	0.25	187 ± 8	468

[a] The fold induction was calculated by dividing the means of the respective β-galactosidase activities by the average value for the uninduced cells (none).
[b] ND, not detectable. β-Galactosidase activity was not quantified when blue color was not detected during the qualitative assay.

TABLE 2. Responses of *czc* promoters to heavy metals

CBA system	Inducer	Growth			Development		
		Metal concn (mM)	Avg β-galactosidase activity ± SD[b]	Fold induction[a]	Metal concn (mM)	Avg β-galactosidase activity ± SD[b]	Fold induction[a]
czc1	None		1 ± 0.1			0.7 ± 0.1	
	$CuSO_4$	0.3	ND		0.060	ND	
	$Ni(NO_3)_2$	1.0	483 ± 48	483	2.0	ND	
	$Zn(NO_3)_2$	0.25	ND		0.1	ND	
	$Co(NO_3)_2$	0.5	618 ± 42	618	1.0	624 ± 37	891
	$Cd(NO_3)_2$	0.1	133 ± 3	133	0.025	221 ± 5	316
	$FeSO_4$	4.0	576 ± 36	576	6.0	38 ± 0.4	54
	$MnSO_4$	0.6	458 ± 43	458	0.8	565 ± 19	807
	$AgNO_3$	0.1	ND		0.01	ND	
	$AuCl_3$	1.0	ND		0.25	ND	
czc2	None		4 ± 0.3			18 ± 0.3[c]	
	$CuSO_4$	0.3	46 ± 4	12	0.060	20 ± 1	1
	$Ni(NO_3)_2$	1.0	ND		2.0	ND	
	$Zn(NO_3)_2$	0.25	19 ± 1	5	0.1	ND	
	$Co(NO_3)_2$	0.5	ND		1.0	ND	
	$Cd(NO_3)_2$	0.1	27 ± 0.4	7	0.025	55 ± 2	3
	$FeSO_4$	6.0	ND		6.0	ND	
	$MnSO_4$	0.6	ND		0.8	ND	
	$AgNO_3$	0.1	ND		0.01	ND	
	$AuCl_3$	1.0	ND		0.25	ND	
czc3	None		27 ± 1			642 ± 9	
	$CuSO_4$	0.3	21 ± 1	1	0.060	56 ± 3	0.1
	$Ni(NO_3)_2$	1.0	5 ± 1	0.2	2.0	97 ± 1	0.2
	$Zn(NO_3)_2$	0.25	9 ± 1	0.3	0.1	48 ± 0.1	0.1
	$Co(NO_3)_2$	0.5	5 ± 1	0.2	1.0	36 ± 1	0.1
	$Cd(NO_3)_2$	0.1	12 ± 1	0.4	0.025	74 ± 5	0.1
	$FeSO_4$	6.0	11 ± 1	0.4	6.0	70.1 ± 0.3	0.1
	$MnSO_4$	0.6	5 ± 1	0.2	0.8	138 ± 6	0.2
	$AgNO_3$	0.1	8 ± 3	0.3	0.01	56 ± 1	0.1
	$AuCl_3$	1.0	11 ± 0.5	0.4	0.25	127 ± 2	0.2

[a] Fold induction was calculated by dividing the means of the respective β-galactosidase activities by the average values for the uninduced cells (none).

[b] ND, not detectable. β-Galactosidase activity was not quantified when blue color was not detected during the qualitative assay.

[c] The maximum level of expression of *czc2* in the absence of copper is reached at 8 h. The presence of copper delayed the maximum up to 24 h (Fig. 4). For comparison, we used samples obtained at 8 h as controls for the assay in the absence of copper and at 24 h when copper was added.

effect on the expression of the three *M. xanthus cus* systems. It should be noted that the responses were not always identical during growth and development (Table 1). Altogether, the obtained results indicate that the three *cus* systems are differentially regulated by copper and other monovalent and/or divalent metals. Furthermore, a different regulation by metals can be observed during growth and development.

The results obtained for the metal response of the Czc systems are shown in Table 2. *czc1* was induced by several divalent metals but not by copper, exhibiting a metal response typical of those of other bacterial Czc systems (21). *czc2* showed a small response to copper, Zn^{2+}, and Cd^{2+}. The upregulation of this *czc* system by copper was clearly detected only during growth but not during development (Fig. 4). Interestingly, *czc3* was constitutively expressed during growth, upregulated by nutrient depletion, and repressed by metals (Fig. 5 and Table 2).

Role of the Cus systems in metal resistance. To analyze whether the Cus systems are involved in metal tolerance, three in-frame deletion mutants were constructed (see Table S1 in the supplemental material). When the three mutants and the WT strain were incubated in liquid CTT medium containing several copper concentrations, it was observed that the copper tolerance of the Δ*cus1* mutant was very similar to that of the

WT strain. However, the Δ*cus3* mutant exhibited a reduced viability at elevated copper concentrations, and the Δ*cus2* mutant was markedly more sensitive than the other three strains to even low metal concentrations (Fig. 6A). These results are in good agreement with the copper induction exhibited by these systems.

Since *M. xanthus* copper adaptation mechanisms are upregulated in cells preincubated with copper (30), mutant cells grown in the presence of this metal should be more sensitive. To test this hypothesis, cells were grown in the presence of 300 μM copper for 24 h. After this preadaptation period, cells were diluted into fresh CTT liquid medium supplemented with higher copper concentrations and incubated for 24 h, when the OD_{600} of the cultures was monitored. As shown in Fig. 6B, only the Δ*cus2* mutant was much more sensitive to copper than the WT strain under these conditions.

In order to elucidate the role of the Cus systems during development, the phenotypes of the mutants and the WT strain plated on CF starvation medium were analyzed. The results obtained with both preadapted and nonpreadapted cells were very similar to those described above during growth, as only the Δ*cus2* mutant turned out to be more sensitive to copper. Details are provided in Fig. S2 in the supplemental material.
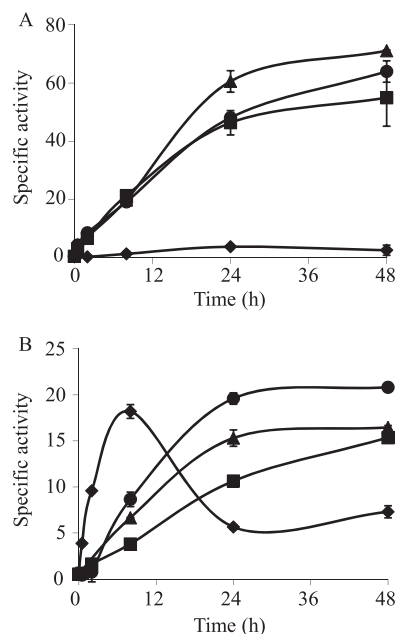
FIG. 4. Copper upregulation of *czc2* during growth (A) and development (B). The strain was grown on CTT agar plates containing 0 μM (◆), 300 μM (■), 600 μM (▲), or 800 μM (●) copper. The copper concentrations added to CF medium during development were 0 μM (◆), 20 μM (■), 40 μM (▲), or 60 μM (●). The specific β-galactosidase activity in the cell extracts was determined as described in Materials and Methods. The results are the averages of data from three different experiments. The error bars indicate standard deviations. Note the differences in the scales.

FIG. 5. Copper upregulation of *czc3* during growth (A) and development (B). The strain was grown on CTT agar plates containing 0 μM (◆), 300 μM (■), 600 μM (▲), or 800 μM (●) copper. The copper concentrations added to CF medium during development were 0 μM (◆), 20 μM (■), 40 μM (▲), or 60 μM (●). The specific β-galactosidase activity in cell extracts was determined as described in Materials and Methods. The results are the averages of data from three different experiments. The error bars indicate standard deviations. Note the differences in the scales.

As the Δ*cus1* and Δ*cus3* mutants did not exhibit a clear sensitivity to copper, we tested whether they could be implicated in conferring resistance to the other metals that are able to induce their expression. When the growth of the Δ*cus1* mutant in liquid CTT medium with Zn^{2+} was monitored, it was observed that these cells tolerated lower metal concentrations than did the WT strain (Fig. 7A). The viability of this mutant was also analyzed with cultures preadapted to the presence of this metal (by preincubation with 0.2 mM Zn^{2+} for 24 h). Under these conditions, the Δ*cus1* mutant exhibited a dramatic reduction in viability compared to that of the WT strain (Fig. 7C). Similar results were observed when the phenotype of the Δ*cus1* mutant grown on starvation medium supplemented with Zn^{2+} was analyzed (Fig. 7B and D).

In contrast, although Cd^{2+} greatly induced the expression of the *cus3* system, no differences between the Δ*cus3* mutant and the WT strain were observed either during growth or during development (data not shown).

Role of the Czc3 system in *M. xanthus* development. Although the same strategy for the construction of the *cus* mutants was used to obtain *czc* deletion mutants, we were unable to obtain the Δ*czc1* and Δ*czc2* strains even after analyzing 96 and 128 Km^s-Gal^r colonies, respectively. All these colonies had reverted to the WT genotype, although 50% were expected to evolve to the corresponding deletion mutant. This negative result suggested that both mutations were lethal. In contrast, the Δ*czc3* mutant could be constructed and phenotypically analyzed. As the express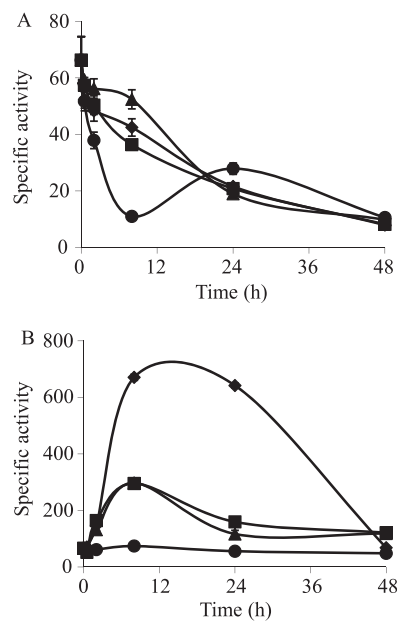ion of this system was repressed by metals (Fig. 5 and Table 2), phenotypic analyses were carried out with no supplementation of metals. Under these conditions, clear differences between the mutant and the WT strain were observed during both growth and development. This mutant grew slower than the WT strain (see Fig. S3 in the supplemental material), exhibiting a generation time of 9 h, while the WT strain duplicated every 6 h. This result is in good agreement with the constitutive expression of *czc3* (Fig. 5A). During development, the mutant delayed aggregation more than 48 h, and the fruiting bodies that originated even after a 96-h incubation were immature (Fig. 8). This result also fits well with the induction of this system on CF starvation medium (Fig. 5B).

DISCUSSION

In the present study the role of the six *M. xanthus* HME-RND systems in copper homeostasis has been examined. These efflux pumps have been described to confer resistance to several metals in some Gram-negative bacteria (5, 7, 14, 23, 25, 31), with the CusCFBA system from *E. coli* (17) being the most investigated. This Cus system is involved in copper homeostasis under conditions of extreme copper stress and is particularly important in anaerobic environments (23). The number of CBA transporters encoded in a genome is highly variable, although most bacteria hold no more than three HME-RND pumps (18). A remarkable exception is *Cupriavidus metallidurans*, a metal-resistant proteobacterium that has 12 HME-RND systems (21). Nevertheless, it seems that when highly
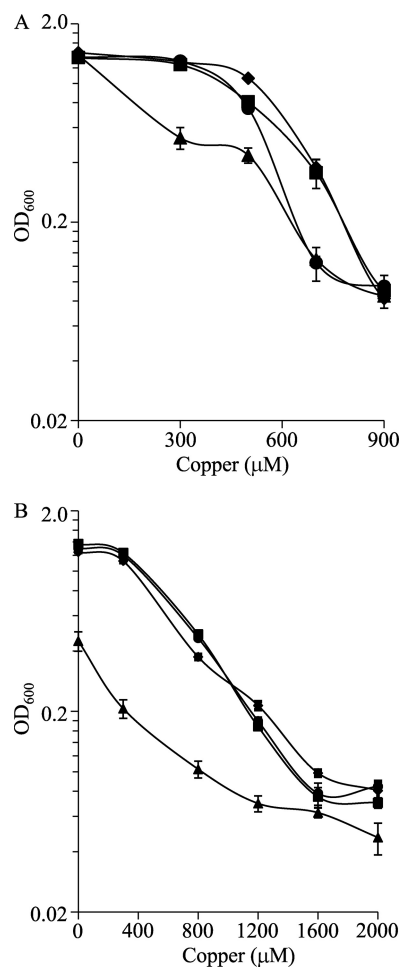
FIG. 6. Copper sensitivities of the *M. xanthus* WT strain (■) and the Δ*cus1* (◆), Δ*cus2* (▲), and Δ*cus3* (●) mutants during growth. (A) Copper tolerance of cells not preadapted to the metal. Cells grown in the absence of copper were diluted to an OD_{600} of 0.05 in fresh CTT liquid medium containing the indicated copper concentrations. The data shown correspond to the OD_{600} monitored at 24 h of incubation. (B) Copper tolerance of cells adapted to copper. Strains were grown in the presence of 300 μM copper prior to dilution into fresh CTT liquid medium containing different copper concentrations. The data are expressed as mentioned above for A and are the averages of data from three experiments. The error bars indicate standard deviations.

related genes are present in a bacterium, usually one is inducible by heavy metal while the rest are silent or constitutively expressed. The fact that *M. xanthus* encodes six CBA transporters to extrude metals, all of which are active under specific circumstances, and that cells are not especially resistant to copper and other metals raises the question of why so many paralogous genes have been maintained in this bacterial genome to participate in metal tolerance.

The results obtained for this report, along with results from other studies of *M. xanthus* MCOs (30) and P_{1B}-type ATPases (15), shed some light on this intriguing question. The variety of expression profiles exhibited by all of the metal-regulated genes of this bacterium indicates that *M. xanthus* cells must be subjected to a fine-tuned control of the metals allocated not only to the cytoplasm but also to the periplasm. Thus, five
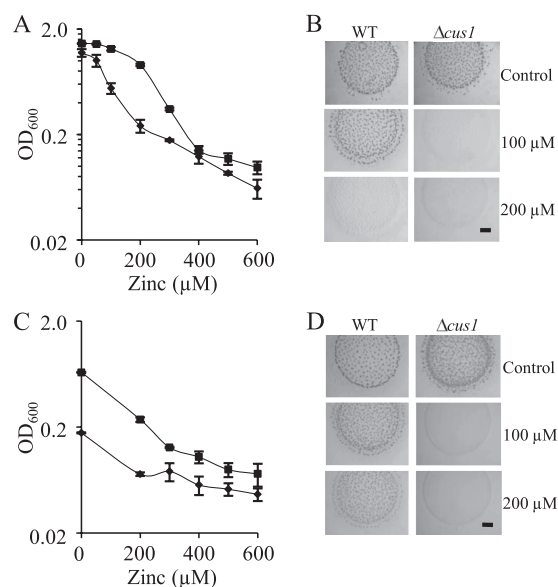

FIG. 7. Zinc sensitivities of the *M. xanthus* WT strain and the Δ*cus1* mutant. (A and B) Zinc tolerance of cells not preadapted to the metal during growth (A) and development (B). (A) Cells grown in the absence of metal were diluted to an OD_{600} of 0.05 in fresh CTT liquid medium containing the indicated zinc concentrations. The data shown correspond to the OD_{600} monitored at 24 h of incubation of WT (■) and Δ*cus1* (◆) strains. (B) Cells not preadapted to zinc were concentrated to an OD_{600} of 15 in TM buffer and spotted onto CF medium containing the indicated zinc concentrations. (C and D) Zinc tolerance of cells adapted to zinc during growth (C) and development (D). (C) The strains were grown in the presence of 200 μM zinc prior to dilution into fresh CTT liquid medium containing different zinc concentrations. The symbols are the same as those indicated above for A. (D) Preadapted cells were concentrated to an OD_{600} of 15 in TM buffer and spotted onto CF medium. The data are the averages of data from three experiments, and the error bars indicate standard deviations (A and C). The pictures were taken after a 96-h incubation, and bars represent 1 mm (B and D).

different expression patterns can be clearly distinguished for the HME-RND transporters, none of which resembles those of the MCOs or the P_{1B}-type ATPases (15, 30). The reason for this fine-adjustment of metal concentrations in the periplasm may be related to the special structure of the *M. xanthus* peptidoglycan, which is required to allow the conversion of the long vegetative rods into coccoid myxospores during development (35). It was shown previously that the accumulation of Cu^+ in the *M. xanthus* periplasm originated from the deletion of some MCOs provoked growing cells to change their bacillary morphology and become spherical forms (30), an obser-
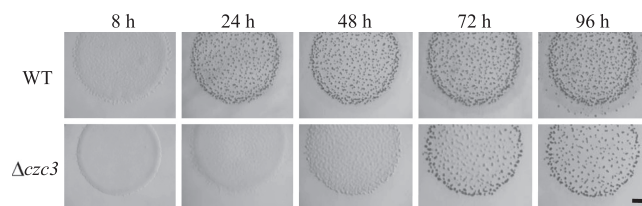

FIG. 8. Development of the WT strain and the Δ*czc3* deletion mutant on CF medium. Pictures were taken at the indicated times. The bar represents 1 mm.

vation that has not been reported for any other rod-shaped bacteria. The results obtained for *M. xanthus* homeostasis suggest that this bacterium copes with changing metal concentrations by using several copies of genes that are differentially regulated by environmental fluctuations. As those paralogs that perform the same function under different conditions have been called ecoparalogs (29), this term can be applied to all *M. xanthus* genes involved in metal homeostasis.

An interesting expression profile (because it cannot be observed for bacteria that do not undergo development) is that exhibited by *czc3*, which is expressed constitutively, induced by starvation, and repressed by the addition of metals. Although the *M. xanthus* MCO *cuoC* is also expressed constitutively and induced by starvation (30), the difference from the *czc3* expression profile lies in the fact that *cuoC* is activated by copper, while *czc3* is repressed. The induction of genes encoding proteins involved in copper homeostasis (and homeostasis of other metals) by starvation suggests that *M. xanthus* cells must also adjust the metal concentration of the dormant myxospores, which would explain why developing cells are much more sensitive to copper than growing cells (30).

Another conclusion that can be deduced from the results obtained for the *M. xanthus* Cus and Czc systems is that not all of them fit into the classification proposed previously by Rensing and Grass (26), based on the sequence motif of TM4 of the RND subunit. Thus, Cus1 resembles a Czc rather than a Cus system. Therefore, it cannot be ruled out that some of the other CBA systems encoded in the *M. xanthus* genome that have not been included in this study could also participate in metal homeostasis.

The differential regulation of HME-RND systems, P_{1B}-ATPases, and MCOs indicates that several transcriptional regulators will participate in the adaptation of *M. xanthus* to changes in the concentrations of copper and other metals. The identification of these factors and the determination of how they sense the fluctuations in metals and nutrients will help to elucidate how this bacterium completes its complex life cycle in soil.

ACKNOWLEDGMENTS

REFERENCES

1. **Argüello, J. M., E. Eren, and M. Gonzalez-Guerrero.** 2007. The structure and function of heavy metal transport P_{1B}-ATPases. Biometals **20:**233–248.
2. **Cho, K., and D. R. Zusman.** 1999. AsgD, a new two-component regulator required for A-signalling and nutrient sensing during early development of *Myxococcus xanthus.* Mol. Microbiol. **34:**268–281.
3. **Finn, R. D., J. Tate, J. Mistry, P. C. Coggill, S. J. Sammut, H. R. Hotz, G. Ceric, K. Forslund, S. R. Eddy, E. L. Sonnhammer, and A. Bateman.** 2008. The Pfam protein families database. Nucleic Acids Res. **36:**D281–D288.
4. **Finney, L. A., and T. V. O'Halloran.** 2003. Transition metal speciation in the cell: insights from the chemistry of metal ion receptors. Science **300:**931–936.
5. **Franke, S., G. Grass, C. Rensing, and D. H. Nies.** 2003. Molecular analysis of the copper-transporting efflux system CusCFBA of *Escherichia coli.* J. Bacteriol. **185:**3804–3812.
6. **Goldberg, M., T. Pribyl, S. Juhnke, and D. H. Nies.** 1999. Energetics and topology of CzcA, a cation/proton antiporter of the resistance-nodulation-cell division protein family. J. Biol. Chem. **274:**26065–26070.
7. **Gupta, A., K. Matsui, J. F. Lo, and S. Silver.** 1999. Molecular basis for resistance to silver cations in *Salmonella.* Nat. Med. **5:**183–188.
8. **Hagen, D. C., A. P. Bretscher, and D. Kaiser.** 1978. Synergism between morphogenetic mutants of *Myxococcus xanthus.* Dev. Biol. **64:**284–296.
9. **Hassan, M. T., D. van der Lelie, D. Springael, U. Romling, N. Ahmed, and M. Mergeay.** 1999. Identification of a gene cluster, *czr,* involved in cadmium and zinc resistance in *Pseudomonas aeruginosa.* Gene **238:**417–425.
10. **Hodgkin, J., and D. Kaiser.** 1977. Cell-to-cell stimulation of movement in nonmotile mutants of *Myxococcus.* Proc. Natl. Acad. Sci. U. S. A. **74:**2938–2942.
11. **Julien, B., A. D. Kaiser, and A. Garza.** 2000. Spatial control of cell differentiation in *Myxococcus xanthus.* Proc. Natl. Acad. Sci. U. S. A. **97:**9098–9103.
12. **Kashefi, K., and P. L. Hartzell.** 1995. Genetic suppression and phenotypic masking of a *Myxococcus xanthus frzF⁻* defect. Mol. Microbiol. **15:**483–494.
13. **Kroos, L., A. Kuspa, and D. Kaiser.** 1986. A global analysis of developmentally regulated genes in *Myxococcus xanthus.* Dev. Biol. **117:**252–266.
14. **Leedjarv, A., A. Ivask, and M. Virta.** 2008. Interplay of different transporters in the mediation of divalent heavy metal resistance in *Pseudomonas putida* KT2440. J. Bacteriol. **190:**2680–2689.
15. **Moraleda-Muñoz, A., J. Pérez, A. L. Extremera, and J. Muñoz-Dorado.** 2010. Expression and physiological role of three *Myxococcus xanthus* copper-dependent P_{1B}-type ATPases during bacterial growth and development. Appl. Environ. Microbiol. **76:**6077–6084.
16. **Moraleda-Muñoz, A., J. Perez, M. Fontes, F. J. Murillo, and J. Muñoz-Dorado.** 2005. Copper induction of carotenoid synthesis in the bacterium *Myxococcus xanthus.* Mol. Microbiol. **56:**1159–1168.
17. **Nies, D. H.** 2007. Bacterial transition metal homeostasis, p. 118–142. *In* D. H. Nies and S. Silver (ed.), Molecular microbiology of heavy metals. Springer-Verlag, Berlin, Germany.
18. **Nies, D. H.** 2003. Efflux-mediated heavy metal resistance in prokaryotes. FEMS Microbiol. Rev. **27:**313–339.
19. **Nies, D. H.** 1999. Microbial heavy-metal resistance. Appl. Microbiol. Biotechnol. **51:**730–750.
20. **Nies, D. H., A. Nies, L. Chu, and S. Silver.** 1989. Expression and nucleotide sequence of a plasmid-determined divalent cation efflux system from *Alcaligenes eutrophus.* Proc. Natl. Acad. Sci. U. S. A. **86:**7351–7355.
21. **Nies, D. H., G. Rehbein, T. Hoffmann, C. Baumann, and C. Grosse.** 2006. Paralogs of genes encoding metal resistance proteins in *Cupriavidus metallidurans* strain CH34. J. Mol. Microbiol. Biotechnol. **11:**82–93.
22. **Nies, D. H., and S. Silver.** 1989. Plasmid-determined inducible efflux is responsible for resistance to cadmium, zinc, and cobalt in *Alcaligenes eutrophus.* J. Bacteriol. **171:**896–900.
23. **Outten, F. W., D. L. Huffman, J. A. Hale, and T. V. O'Halloran.** 2001. The independent *cue* and *cus* systems confer copper tolerance during aerobic and anaerobic growth in *Escherichia coli.* J. Biol. Chem. **276:**30670–30677.
24. **Pena, M. M., J. Lee, and D. J. Thiele.** 1999. A delicate balance: homeostatic control of copper uptake and distribution. J. Nutr. **129:**1251–1260.
25. **Pontel, L. B., M. E. Audero, M. Esparíz, S. K. Checa, and F. C. Soncini.** 2007. GolS controls the response to gold by the hierarchical induction of *Salmonella*-specific genes that include a CBA efflux-coding operon. Mol. Microbiol. **66:**814–825.
26. **Rensing, C., and G. Grass.** 2003. *Escherichia coli* mechanisms of copper homeostasis in a changing environment. FEMS Microbiol. Rev. **27:**197–213.
27. **Rensing, C., T. Pribyl, and D. H. Nies.** 1997. New functions for the three subunits of the CzcCBA cation-proton antiporter. J. Bacteriol. **179:**6871–6879.
28. **Sambrook, J., and D. W. Russell.** 2001. Molecular cloning: a laboratory manual, 3rd ed. Cold Spring Harbor Laboratory Press, Cold Spring Harbor, NY.
29. **Sanchez-Perez, G., A. Mira, G. Nyiro, L. Pasic, and F. Rodriguez-Valera.** 2008. Adapting to environmental changes using specialized paralogs. Trends Genet. **24:**154–158.
30. **Sanchez-Sutil, M. C., N. Gomez-Santos, A. Moraleda-Muñoz, L. O. Martins, J. Perez, and J. Muñoz-Dorado.** 2007. Differential expression of the three multicopper oxidases from *Myxococcus xanthus.* J. Bacteriol. **189:**4887–4898.
31. **Schmidt, T., and H. G. Schlegel.** 1994. Combined nickel-cobalt-cadmium resistance encoded by the *ncc* locus of *Alcaligenes xylosoxidans* 31A. J. Bacteriol. **176:**7045–7054.
32. **Tseng, T. T., K. S. Gratwick, J. Kollman, D. Park, D. H. Nies, A. Goffeau, and M. H. Saier, Jr.** 1999. The RND permease superfamily: an ancient, ubiquitous and diverse family that includes human disease and development proteins. J. Mol. Microbiol. Biotechnol. **1:**107–125.
33. **Ueki, T., S. Inouye, and M. Inouye.** 1996. Positive-negative KG cassettes for construction of multi-gene deletions using a single drug marker. Gene **183:**153–157.
34. **Waldron, K. J., J. C. Rutherford, D. Ford, and N. J. Robinson.** 2009. Metalloproteins and metal sensing. Nature **460:**823–830.
35. **Whitworth, D. E (ed.).** 2008. Myxobacteria. Multicellularity and differentiation. ASM Press, Washington, DC.